




Accurate prediction of ^{195}Pt -NMR chemical shifts for hydrolysis products of $[\text{PtCl}_6]^{2-}$ in acidic and alkaline aqueous solutions by non-relativistic DFT computational protocols

Athanassios C. Tsipis & Ioannis N. Karapetsas

To cite this article: Athanassios C. Tsipis & Ioannis N. Karapetsas (2015) Accurate prediction of ^{195}Pt -NMR chemical shifts for hydrolysis products of $[\text{PtCl}_6]^{2-}$ in acidic and alkaline aqueous solutions by non-relativistic DFT computational protocols, Journal of Coordination Chemistry, 68:21, 3788-3804, DOI: [10.1080/00958972.2015.1083095](https://doi.org/10.1080/00958972.2015.1083095)


To link to this article: <http://dx.doi.org/10.1080/00958972.2015.1083095>

 View supplementary material [↗](#)

 Accepted author version posted online: 21 Aug 2015.
Published online: 11 Sep 2015.

 Submit your article to this journal [↗](#)

 Article views: 47

 View related articles [↗](#)

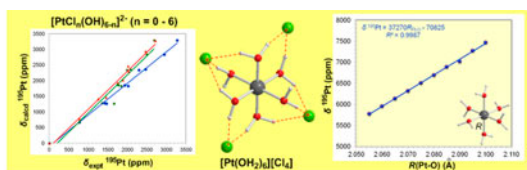
 View Crossmark data [↗](#)

Accurate prediction of ^{195}Pt -NMR chemical shifts for hydrolysis products of $[\text{PtCl}_6]^{2-}$ in acidic and alkaline aqueous solutions by non-relativistic DFT computational protocols

ATHANASSIOS C. TSIPIS* and IOANNIS N. KARAPETSAS

Laboratory of Inorganic and General Chemistry, Department of Chemistry, University of Ioannina, Ioannina, Greece

(Received 10 May 2015; accepted 16 July 2015)



The ^{195}Pt -NMR chemical shifts of all possible hydrolysis products of $[\text{PtCl}_6]^{2-}$ in acidic and alkaline aqueous solutions are calculated employing simple non-relativistic density functional theory computational protocols. Particularly, the GIAO-PBE0/SARC-ZORA(Pt) U 6-31 + G(d)(E) computational protocol augmented with the universal continuum solvation model (SMD) performs the best for calculation of the ^{195}Pt -NMR chemical shifts of the Pt(IV) complexes existing in acidic and alkaline aqueous solutions of $[\text{PtCl}_6]^{2-}$. Excellent linear plots of $\delta_{\text{calcd}}(^{195}\text{Pt})$ chemical shifts versus $\delta_{\text{expt}}(^{195}\text{Pt})$ chemical shifts and $\delta_{\text{calcd}}(^{195}\text{Pt})$ versus the natural atomic charge Q_{Pt} are obtained. Very small changes in the Pt–Cl and Pt–O bond distances of the octahedral $[\text{PtCl}_6]^{2-}$, $[\text{Pt}(\text{OH})_6]^{2-}$, and $[\text{Pt}(\text{OH}_2)_6]^{4+}$ complexes have significant influence on the computed $\sigma_{\text{iso}}^{195}\text{Pt}$ magnetic shielding tensor elements of the anionic $[\text{PtCl}_6]^{2-}$ and the computed $\delta^{195}\text{Pt}$ chemical shifts of $[\text{Pt}(\text{OH})_6]^{2-}$ and $[\text{Pt}(\text{OH}_2)_6]^{4+}$. An increase of the Pt–Cl and Pt–O bond distances by 0.001 Å (1 mÅ) is accompanied by a downfield shift increment of 17.0, 19.4, and 37.6 ppm mÅ $^{-1}$, respectively. Counter-anion effects in the case of the highly positive charged complexes drastically improve the accuracy of the calculated ^{195}Pt chemical shifts providing values very close to the experimental ones.

Keywords: ^{195}Pt -NMR; DFT calculations; Prediction of ^{195}Pt chemical shifts; Hydrolysis products of $[\text{PtCl}_6]^{2-}$ in aqueous solutions

1. Introduction

The speciation and preferential extraction of Pt(IV)-mixed halide complexes in acidic aqueous solutions have been studied by ^{195}Pt -NMR spectroscopy [1]. Dependent on the solution

*Corresponding author. Email: attsipis@uoi.gr

conditions (platinum and halide content, pH, and temperature), the $[\text{PtCl}_6]^{2-}$ species in aqueous solutions may undergo varying degrees of aquation and/or hydrolysis, leading to several $[\text{PtCl}_n(\text{H}_2\text{O})_{6-n}]^{4-n}$ and $[\text{PtCl}_n(\text{OH})_{6-n}]^{2-}$ ($n = 1-5$) species [2]. Goodfellow *et al.* [3] initially produced all 10 complexes of the type $[\text{PtCl}_n(\text{OH})_{6-n}]^{2-}$ ($n = 0-6$) in aqueous solution by a combination of methods: the *homoleptic* complexes, $[\text{PtCl}_6]^{2-}$ and $[\text{Pt}(\text{OH})_6]^{2-}$, were prepared by simply dissolving the appropriate commercially available salts, Na_2PtCl_6 and $\text{Na}_2\text{Pt}(\text{OH})_6$, in water, while the five complexes $[\text{PtCl}_n(\text{OH})_{6-n}]^{2-}$, where $n = 1-3$, were generated by adding a further equivalent of Na_2PtCl_6 salt to an aqueous solution of Na_2PtCl_6 with five equivalents of sodium hydroxide that had been allowed to age for seven days at 288 K. The three remaining complexes, $[\text{PtCl}_5(\text{OH})]^{2-}$ and the stereoisomers *cis/trans*- $[\text{PtCl}_4(\text{OH})_2]^{2-}$, were produced by boiling a solution of Ag_2PtCl_6 in water and then adjusting to pH 10. It is interesting to note that, apparently, it is possible to isolate some of these complexes as pure salts [4-6]. According to Kramer and Koch [7], the addition of an appropriate excess of sodium hydroxide to a concentrated aqueous solution (*ca.* 0.4 M) of H_2PtCl_6 or Na_2PtCl_6 (or dissolving either of these in a sufficiently alkaline solution) results in $[\text{PtCl}_n(\text{OH})_{6-n}]^{2-}$ ($n = 0-6$).

A detailed analysis of the $^{35}\text{Cl}/^{37}\text{Cl}$ isotope shifts induced in the 128.8 MHz $^{195}\text{Pt-NMR}$ resonances of the $[\text{PtCl}_n(\text{H}_2\text{O})_{6-n}]^{4-n}$ and $[\text{PtCl}_n(\text{OH})_{6-n}]^{2-}$ ($n = 1-5$) complex ions showed that all species in the series $[\text{PtCl}_n(\text{H}_2\text{O})_{6-n}]^{4-n}$ ($n = 2-6$) display unique $^{35/37}\text{Cl}$ isotope effects [7-9]. These effects result in a unique "fine-structure" of each individual resonance, which constitutes an unambiguous spectroscopic "fingerprint" characteristic of the structure of the octahedral platinum(IV) complex, provided $^{195}\text{Pt-NMR}$ are recorded at optimum magnetic field homogeneity and carefully controlled temperature (293 ± 0.1 K).

The speciation and hydration/solvation of $[\text{PtX}_6]^{2-}$ ($X = \text{Cl}, \text{Br}$) anions in solution have also been investigated employing a combination of $^{195}\text{Pt-NMR}$ together with density functional theory (DFT) calculations and molecular dynamics simulations [10]. The zero-point vibrationally averaged structures for $[\text{Pt}^{35}\text{Cl}_6]^{2-}$ and $[\text{Pt}^{37}\text{Cl}_6]^{2-}$, the $[\text{Pt}^{35}\text{Cl}_n^{37}\text{Cl}_{5-n}(\text{H}_2\text{O})]^-$ ($n = 0-5$), *cis*- $(\text{Pt}^{35}\text{Cl}_n^{37}\text{Cl}_{4-n}(\text{H}_2\text{O})_2)$ ($n = 0-4$), and *fac*- $[(\text{Pt}^{35}\text{Cl}_n\text{Cl}_{3-n}(\text{H}_2\text{O})_3)]^+$ ($n = 0-3$) isotopologs and isotopomers were calculated at the PBE0/SDD/6-31* level [11, 12]. The calculated $^{195}\text{Pt-NMR}$ shielding constants at the ZORA-SO/PW91/QZ4P/TZ2P level were used to evaluate the corresponding $^{35/37}\text{Cl}$ isotope shifts in the experimental $^{195}\text{Pt-NMR}$ spectra. The observed effects are reproduced reasonably well in terms of qualitative trends, but quantitative agreement with experiment is not yet achieved. Ismail *et al.* [13] indicated that the isotope effect may be a new way to characterize $[\text{PtCl}_n(\text{H}_2\text{O})_{6-n}]^{4-n}$ ($n = 1-5$) and $[\text{PtCl}_n(\text{OH})_{6-n}]^{2-}$ ($n = 1-5$) complexes. Although according to molecular orbital theory, the existence of $[\text{Pt}(\text{H}_2\text{O})_6]^{4+}$ is possible and synthesis of $[\text{Pt}(\text{H}_2\text{O})_6]^{4+}$ has not been reported. However, very recently Murray [14] reported the synthesis of $[\text{Pt}(\text{H}_2\text{O})_6]^{4+}$ complex in strong acidic solution and its characterization by $^{195}\text{Pt-NMR}$ spectroscopy. All of the $[\text{PtCl}_n(\text{H}_2\text{O})_{6-n}]^{4-n}$ ($n = 1-5$) *aqua* ions are formed by driving aquation of $[\text{PtCl}_6]^{2-}$ via addition of AgClO_4 to an aqueous solution of $[\text{PtCl}_6]^{2-}$.

Despite the numerous experimental applications of $^{195}\text{Pt-NMR}$ spectroscopy, theoretical predictions of the ^{195}Pt chemical shifts for the $[\text{PtCl}_n(\text{H}_2\text{O})_{6-n}]^{4-n}$ ($n = 1-5$) and $[\text{PtCl}_n(\text{OH})_{6-n}]^{2-}$ ($n = 1-5$) complexes are limited. However, it was shown that the calculated δ (^{195}Pt) chemical shifts for species that contain coordinated *hydroxide* or *aqua* ligands, using DFT methods, deviate from experimental results, possibly due to hydrogen bonding effects not accounted for by these methods [10].

Recently, an exhaustive assessment of the performance of diverse computational protocols based on DFT methods without including relativistic and spin-orbit effects

for the computation of ^{195}Pt chemical shifts for a series of Pt(II) and Pt(IV) anticancer agents [15] revealed the good performance of the GIAO-PBE0/SARC-ZORA(Pt) U 6-31 + G(d)(E) (E = main group element) computational protocol combined with either the Polarizable Continuum Model (PCM) solvation model or the universal continuum solvation model (SMD) for aqueous solutions. Herein, we extend the applicability and generality of the GIAO-PBE0/SARC-ZORA(Pt) U BS(E)/(PCM or SMD) (BS = 6-31 + G(d) or 6-31G(d,p); E = main group element) computational protocols for the prediction of δ ^{195}Pt chemical shifts for all possible hydrolysis products of $[\text{PtCl}_6]^{2-}$ in acidic and alkaline aqueous solutions formulated as $[\text{PtCl}_n(\text{H}_2\text{O})_{6-n}]^{4-n}$ and $[\text{PtCl}_n(\text{OH})_{6-n}]^{2-}$ ($n = 0-6$), respectively.

2. Computational details

All calculations were performed using the Gaussian09 program suite [16]. The geometries of all stationary points were fully optimized, without symmetry constraints, employing the 1999 hybrid functional of Perdew, Burke, and Ernzerhof [17–23] (denoted as PBE0) as implemented in the Gaussian09 program suite. For the geometry optimizations, we used the SARC-ZORA basis [24, 25] for Pt and the 6-31 + G(d) or 6-31G(d,p) basis set for all other main group elements E were tested. The selection of these basis sets for the E elements was based on the recently reported work on the role of the basis set in the prediction of the structure and reactivity of cisplatin by Dos Santos and co-workers [26]. The SARC basis set is a family of segmented all-electron relativistically contracted basis sets for use in conjunction with the Douglas-Kroll Hamiltonian and Zeroth-Order Regular Approximation (ZORA) scalar relativistic Hamiltonians [24, 25]. Although it seems to be a theoretical inconsistency in the use of the SARC-ZORA basis sets for non-relativistic calculations, the fact that the SARC-ZORA basis sets are optimized for the ZORA Hamiltonian does not mean that they “must” be used with the ZORA Hamiltonian. They are fairly big all-electron basis sets that are flexible enough by construction to be of general use. As a matter of fact, they are probably even bigger than necessary when used in non-relativistic calculations [27]. Moreover, it should be noticed that, despite the importance of relativistic effects for the heavy atoms, orbital exponents optimized through the well-tempered scheme for non-relativistic calculations can be carried over to relativistic calculations to produce wave functions close to the relativistic HF limit [28, 29]. Hereafter, the method used in DFT calculations is abbreviated as PBE0/SARC-ZORA(Pt) U 6-BS(E). All stationary points have been identified as minima. Solvent effects were accounted for by means of the PCM using the integral equation formalism variant being the default self-consistent reaction field method [30] and the universal continuum solvation model based on solute electron density called SMD [31]. Magnetic shielding tensors have been computed with the GIAO (gauge-including atomic orbitals) DFT method [32, 33] as implemented in the Gaussian09 series of programs. To be consistent with the experimental data available, we report ^{195}Pt -NMR chemical shifts with respect to $[\text{PtCl}_6]^{2-}_{(\text{aq})}$ reference compound, using the chemical shift definition [34]: $\delta = (\sigma_{\text{ref}} - \sigma) / (1 - \sigma_{\text{ref}})$ in its approximate form $\delta \approx (\sigma_{\text{ref}} - \sigma)$. Shielding constants and chemical shifts are given in ppm.

3. Results and discussion

3.1. σ^{iso} ¹⁹⁵Pt Magnetic shielding tensor elements of anionic [PtCl₆]²⁻, [HPtCl₆]⁻ and neutral H₂PtCl₆ reference compounds in aqueous solutions

Taking into account that structural effects combined with the presence of solvent influence significantly the ¹⁹⁵Pt-NMR parameters [35–37], first we optimized the structure of the anionic [PtCl₆]²⁻, [HPtCl₆]⁻ and neutral H₂PtCl₆ (both *cis*- and *trans*-isomers) reference compounds in aqueous solutions employing the PCM and SMD solvation models. Hydrogen hexachloroplatinate(IV), H₂PtCl₆ (also called chloroplatinic acid), is one of the most frequently used compounds for the preparation of supported platinum catalysts. H₂PtCl₆ is a strong acid that undergoes rapid and extensive hydrolysis. While the degree of dissociation of the diprotic acid is unclear, it is generally agreed that chloroplatinic acid solutions are mildly acidic [38]. The acidic properties of H₂PtCl₆ studied a long time ago by Maatman and Addink [39] showed that the two hydrogens are equivalent and provided no evidence that [HPtCl₆]⁻ existed in solutions. On the other hand, H₂PtCl₆ has been used as an external reference standard; an example is given in Refs. [40, 41]. The isotropic shielding tensor elements, σ^{iso} ¹⁹⁵Pt (ppm) of the anionic [PtCl₆]²⁻, [HPtCl₆]⁻, and neutral H₂PtCl₆ reference compounds along with the *R*(Pt–Cl) bond distances and the natural atomic charges on Pt central atom, *Q*_{Pt}, calculated at the PBE0/SARC-ZORA(Pt) U BS(Cl) (BS = 6-31 + G(d) or 6-31G(d,p)) levels in aqueous solutions combined with the PCM or SMD solvation models are given in table 1. The optimized structures of the anionic [HPtCl₆]⁻ and neutral H₂PtCl₆ compounds in aqueous solutions are shown in figures S1 and S2.

The data in table 1 shows that the calculated σ^{iso} ¹⁹⁵Pt magnetic shielding tensor elements for [PtCl₆]²⁻, [HPtCl₆]⁻, and H₂PtCl₆ reference compounds are strongly affected by solvation with the changes observed being also sensitive to the basis sets used for the main group elements E, while the solvation models used have lower effect. A downfield shift of 10 (42), 19 (25), 46 (20), and 7 (24) ppm is observed on going from the PCM to SMD solvation model for [PtCl₆]²⁻, [HPtCl₆]⁻, *cis*-H₂PtCl₆, and *trans*-H₂PtCl₆ reference compounds, respectively, calculated at the PBE0/SARC-ZORA(Pt) U 6-31+G(d)(Cl) and PBE0/SARC-ZORA(Pt) U 6-31G(d,p)(Cl) (figures in parentheses) levels. Appreciable upfield shifts of the σ^{iso} ¹⁹⁵Pt magnetic shielding tensors of 113–380 ppm are also observed for reference compounds on going from 6-31+G(d) to 6-31G(d,p) basis set used for Cl.

Table 1. σ^{iso} ¹⁹⁵Pt magnetic shielding tensor elements (in ppm) for the anionic [PtCl₆]²⁻, [HPtCl₆]⁻ and neutral H₂PtCl₆ reference compounds calculated at the GIAO-PBE0/SARC-ZORA(Pt) U 6-31 + G(d)(Cl) and GIAO-PBE0/SARC-ZORA(Pt) U 6-31G(d,p)(Cl) (figures in parentheses) levels in aqueous solutions employing the PCM and SMD solvation models, the *R*(Pt–Cl) bond distances (in Å) and the natural atomic charges on Pt, *Q*_{Pt}.

Compound	σ^{iso} ¹⁹⁵ Pt		<i>R</i> (Pt–Cl) ^a		<i>Q</i> _{Pt}	
	PCM	SMD	PCM	SMD	PCM	SMD
[PtCl ₆] ²⁻	-1280 (-1628)	-1290 (-1670)	2.396 (2.398)	2.394 (2.395)	-0.010 (-0.017)	0.005 (-0.0006)
[HPtCl ₆] ⁻	-952 (-1171)	-971 (-1200)	2.398 (2.398)	2.398 (2.398)	-0.026 (-0.032)	-0.016 (-0.021)
<i>cis</i> -H ₂ PtCl ₆	-617 (-730)	-571 (-710)	2.405 (2.405)	2.404 (2.405)	-0.026 (-0.029)	-0.028 (-0.028)
<i>trans</i> - H ₂ PtCl ₆	-1000 (-1146)	-976 (-1153)	2.385 (2.385)	2.385 (2.385)	-0.073 (-0.075)	-0.070 (-0.071)

^aFor [HPtCl₆]⁻, *cis*-H₂PtCl₆, and *trans*-H₂PtCl₆ compounds the average *R*(Pt–Cl) bond distances are given.

As can be seen from table 1, protonation of the anionic $[\text{PtCl}_6]^{2-}$ complex strongly affects the $\sigma^{\text{iso } 195}\text{Pt}$ magnetic shielding tensors introducing appreciable downfield shifts; higher downfield shifts are obtained for *cis*- H_2PtCl_6 . Notice that, for both isomers, the downfield shifts observed depend on the basis sets and the solvation models used. The downfield shifts observed could be accounted for by the structural changes introduced by the protonation of the $[\text{PtCl}_6]^{2-}$ complex (figures S1 and S2). In $[\text{HPtCl}_6]^-$ and *cis*- H_2PtCl_6 , the Pt–Cl bonds are elongated with respect to the Pt–Cl bonds of $[\text{PtCl}_6]^{2-}$, and the elongation being higher in *cis*- H_2PtCl_6 than $[\text{HPtCl}_6]^-$. On the other hand, in *trans*- H_2PtCl_6 the Pt–Cl bonds are shortened with respect to the Pt–Cl bonds of the $[\text{PtCl}_6]^{2-}$ complex. The Pt–ClH bonds between the Pt and the protonated chloride ligands in $[\text{HPtCl}_6]^-$ are elongated by 0.145 Å with respect to the Pt–Cl bonds of $[\text{PtCl}_6]^{2-}$. These structural changes are mirrored on the natural atomic charges of the central Pt, Q_{Pt} , calculated by Natural Bond Orbital analysis method at the PBE0/SARC-ZORA(Pt) U BS(E) levels (table 1). In summary, it can be concluded that *the calculated $\sigma^{\text{iso } 195}\text{Pt}$ magnetic shielding tensors for $[\text{PtCl}_6]^{2-}$, $[\text{HPtCl}_6]^-$ and H_2PtCl_6 reference compounds are primarily associated with the natural atomic charge Q_{Pt} , which is regulated by the coordination sphere of the complex.* To probe further this conclusion, we performed calculations of the $\sigma^{\text{iso } 195}\text{Pt}$ magnetic shielding and the natural atomic charges Q_{Pt} of $[\text{PtCl}_6]^{2-}$ as a function of the Pt–Cl bond distances. The variations of $\sigma^{\text{iso } 195}\text{Pt}$ and Q_{Pt} as a function of the $R(\text{Pt}–\text{Cl})$ bond distances in the $[\text{PtCl}_6]^{2-}$ reference compound calculated by the PBE0/SARC-ZORA(Pt) U 6-31 + G(d)(Cl)/SMD computational protocol are given in table S1.

Excellent linear relationships shown in figure 1 are obtained for the $\sigma^{\text{iso } 195}\text{Pt}$ versus R (Pt–Cl) and $\sigma^{\text{iso } 195}\text{Pt}$ versus Q_{Pt} correlations. Interestingly, the electron density on the central Pt is directly related with the $R(\text{Pt}–\text{Cl})$ bond distance and therefore the $R(\text{Pt}–\text{Cl})$ bond distance is the decisive factor that determines the electron density on Pt and consequently the $\sigma^{\text{iso } 195}\text{Pt}$ magnetic shielding tensor elements are directly related to the electron density on the central Pt.

Perusal of figure 1 and table S1 reveals that very small changes in the Pt–Cl bond distances have a significant influence on the computed $\sigma^{\text{iso } 195}\text{Pt}$ magnetic shielding tensor elements of the $[\text{PtCl}_6]^{2-}$ reference compound. In effect an increase of the Pt–Cl bond distance by 0.001 Å (1 mÅ) is accompanied by a downfield shift increment of 17 (ppm mÅ⁻¹). The

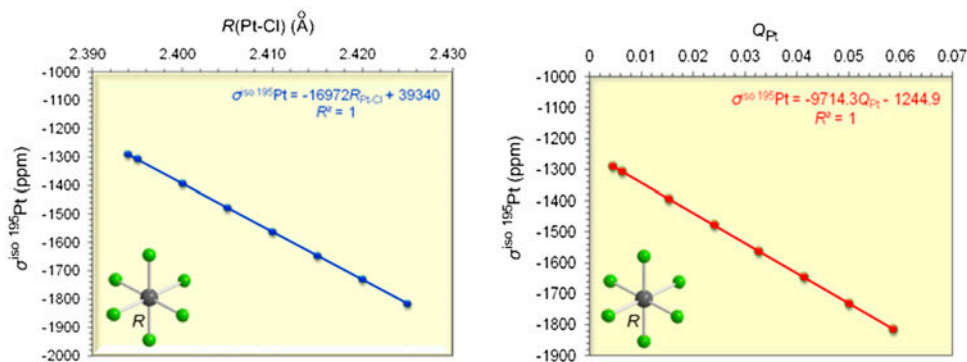


Figure 1. $\sigma^{\text{iso } 195}\text{Pt}$ vs. $R(\text{Pt}–\text{Cl})$ and $\sigma^{\text{iso } 195}\text{Pt}$ vs. Q_{Pt} linear relationships for the anionic $[\text{PtCl}_6]^{2-}$ complex calculated at the PBE0/SARC-ZORA(Pt) U 6-31 + G(d)(Cl) level in aqueous solutions combined with the SMD solvation model.

sensitivity of the chemical shift to the Pt–ligand bond distance has previously been described for $[\text{PtCl}_x\text{Br}_{6-x}]^{2-}$ and $[\text{PtX}_{6-n}\text{Y}_n]^{2-}$ ($X = \text{Cl}, \text{Br}$ and $Y = \text{F}, \text{I}$) series of complexes [42, 43]. Scalar relativistic ZORA with TZP and LDA approximation calculations on $[\text{PtCl}_x\text{Br}_{6-x}]^{2-}$ and $[\text{PtX}_{6-n}\text{Y}_n]^{2-}$ ($X = \text{Cl}, \text{Br}$ and $Y = \text{F}, \text{I}$) series of complexes predicted analogous chemical shift increments with increasing Pt–X bond distances of 15.0 (ppm/mÅ) for $[\text{PtCl}_x\text{Br}_{6-x}]^{2-}$ [42] and 18.3 (ppm/mÅ) for $[\text{PtCl}_6]^{2-}$ [43]. The downfield shift increment could be explained by taking into account the electron density on Pt, as it is expressed by the computed natural atomic charge Q_{Pt} , for the Q_{Pt} is directly related with the Pt–Cl bond length and the $\sigma^{\text{iso}} \text{ } ^{195}\text{Pt}$ magnetic shielding. Thus, as the Pt–Cl bond length increases, the electron density on Pt decreases (Q_{Pt} increases) and, therefore, the platinum is deshielded giving downfield shift increments. Considering the high sensitivity of the computed $\sigma^{\text{iso}} \text{ } ^{195}\text{Pt}$ magnetic shielding for the reference compound on the factors outlined above, *accurate $\delta \text{ } ^{195}\text{Pt}$ chemical shifts for platinum compounds could be predicted if the calculations of the $\sigma^{\text{iso}} \text{ } ^{195}\text{Pt}$ magnetic shielding for the selected reference compound are performed strictly under the same conditions.*

The sensitivity of the $\sigma^{\text{iso}} \text{ } ^{195}\text{Pt}$ magnetic shielding to the Pt–Cl bond distances of $[\text{PtCl}_6]^{2-}$ could be related with the sensitivity of the $\sigma^{\text{iso}} \text{ } ^{195}\text{Pt}$ magnetic shielding to relativistic effects. CP-aiMD and ADF-COSMO calculations [37] predicted Pt–Cl bond lengths for the $[\text{PtCl}_6]^{2-}$ reference compound of 2.38 ± 0.02 and 2.375 \AA , respectively, which compare well with the PBE0/SARC-ZORA(Pt) U 6-31 + G(d)(Cl)/SMD value of 2.394 \AA . Scalar relativistic ZORA with TZP and LDA approximation calculations [42] predicted a Pt–Cl bond length of 2.341 \AA being closer to the experimental values of 2.316 and 2.330 \AA obtained by EXAFS and diffraction methods [44, 45]. It should be noticed that solution structures involve elongated Pt–ligand bonds compared to the solid state structures, because of the solvation effects and, therefore, any comparison of the structures is meaningless.

A series of hydrolysis products with general formula $[\text{PtCl}_n(\text{OH})_m(\text{H}_2\text{O})_{6-n-m}]^{2-n-m}$ ($n, m = 0\text{--}6$) exist in aqueous solutions of H_2PtCl_6 at different H_2PtCl_6 concentrations, pH values, chloride ion concentrations, and time [35, 38]. In the next sections, we analyze the calculated ^{195}Pt -NMR chemical shifts of all possible $[\text{PtCl}_n(\text{OH})_m(\text{H}_2\text{O})_{6-n-m}]^{2-n-m}$ ($n, m = 0\text{--}6$) complexes in aqueous acidic and alkaline solutions.

3.2. ^{195}Pt -NMR Chemical shifts of the $[\text{PtCl}_n(\text{OH})_{6-n}]^{2-}$ ($n = 1\text{--}6$) complexes in aqueous solutions

^{195}Pt -NMR chemical shifts for all possible $[\text{PtCl}_n(\text{OH})_{6-n}]^{2-}$ ($n = 1\text{--}6$) complexes as calculated at the GIAO-PBE0/SARC-ZORA(Pt)U BS(E) (BS = 6-31 + G(d) or 6-31G(d,p)) level in aqueous solutions employing the PCM and SMD solvation models are compiled in table 2. An inspection of the calculated $\delta_{\text{calcd}} \text{ } ^{195}\text{Pt}$ and experimental $\delta_{\text{exptl}} \text{ } ^{195}\text{Pt}$ chemical shifts (table 2) reveals that the PBE0/SARC-ZORA(Pt) U 6-31 + G(d)(E)/SMD computational protocol is the best performer in the calculation of $\delta \text{ } ^{195}\text{Pt}$ chemical shifts of the $[\text{PtCl}_n(\text{OH})_{6-n}]^{2-}$ ($n = 0\text{--}6$) complexes giving the lower mean absolute percentage deviation of the calculated from the experimental values (7.4%). The estimated error bars range from 13 to 205 ppm with the mean error bar being 108 ppm.

Recently, Sutter and Autschbach [46] studied the ^{195}Pt -, ^{14}N -, and ^{15}N -NMR data for five platinum azido (N_3^-) complexes using relativistic DFT. However, high error bars of 512–636 ppm of the calculated from the experimental values are observed for the azido Pt(IV) complexes. The authors stated that even for such high error bars, the agreement of the

Table 2. ^{195}Pt -NMR chemical shifts (in ppm) for all possible $[\text{PtCl}_n(\text{OH})_{6-n}]^{2-}$ ($n = 0-6$) complexes referenced to $[\text{PtCl}_6]^{2-}$, percent deviation, Dev (%) and error bars (in ppm) calculated at the GIAO-PBE0/SARC-ZORA (Pt)U 6-31 + G(d)(Cl) and GIAO-PBE0/SARC-ZORA(Pt)U 6-31G(d,p)(Cl) (figures in parentheses) levels in aqueous solution employing the PCM and SMD solvation models along with experimental values available.

Compound	$\delta_{\text{calcd}}^{195\text{Pt}^a}$		$\delta_{195\text{Pt}}^{\text{exptl}^b}$	Dev (%)		Error bars	
	PCM	SMD		PCM	SMD	PCM	SMD
$[\text{PtCl}_6]^{2-}$	-1280 (-1628)	-1290 (-1670)	0				
$[\text{PtCl}_5(\text{OH})]^{2-}$	780 (753)	766 (762)	666	17.1 (13.1)	15.0 (14.4)	114 (87)	100 (96)
<i>cis</i> - $[\text{PtCl}_4(\text{OH})_2]^{2-}$	1457 (1413)	1417 (1351)	1281	13.7 (10.3)	10.6 (5.5)	176 (132)	136 (70)
<i>trans</i> - $[\text{PtCl}_4(\text{OH})_2]^{2-}$	1654 (1669)	1468 (1459)	1263	31.0 (32.1)	16.2 (15.5)	391 (406)	205 (196)
<i>fac</i> - $[\text{PtCl}_3(\text{OH})_3]^{2-}$	1992 (1876)	1934 (1772)	1854	7.4 (1.2)	4.3 (-4.4)	138 (22)	80 (82)
<i>mer</i> - $[\text{PtCl}_3(\text{OH})_3]^{2-}$	2176 (2135)	2022 (1840)	1831	18.8 (16.6)	10.4 (0.5)	345 (304)	191 (9)
<i>cis</i> - $[\text{PtCl}_2(\text{OH})_4]^{2-}$	2542 (2394)	2466 (2078)	2364	7.5 (1.3)	4.3 (-12.1)	178 (30)	102 (286)
<i>trans</i> - $[\text{PtCl}_2(\text{OH})_4]^{2-}$	2732 (2641)	2297 (1992)	2340	16.8 (12.9)	-1.8 (-14.9)	392 (301)	43 (348)
$[\text{PtCl}(\text{OH})_5]^{2-}$	2933 (2686)	2945 (2499)	2840	3.3 (-5.4)	3.7 (-12.0)	93 (154)	105 (341)
$[\text{Pt}(\text{OH})_6]^{2-}$	3225 (2850)	3280 (2685)	3293	-2.1 (-13.5)	-0.4 -18.5	68 (443)	13 (608)

^aThe calculated σ^{iso} ^{195}Pt magnetic shielding tensor elements are given for the $[\text{PtCl}_6]^{2-}$ reference compound.

^bFrom Ref. [3].

calculations with experiment can be considered acceptable when keeping in mind the very large chemical shift range of Pt. According to the authors, error bars that are reliably below 100 ppm would likely require a high-level correlated wave function method within an all-electron relativistic framework, which is presently out of reach. The estimated mean error bar of 108 ppm for the $[\text{PtCl}_n(\text{OH})_{6-n}]^{2-}$ ($n = 0-6$) complexes illustrates the good performance of the PBE0/SARC-ZORA(Pt) U 6-31 + G(d)(E)/SMD computational protocol. The $[\text{PtCl}_5(\text{OH})]^{2-}$, $[\text{cis-PtCl}_4(\text{OH})_2]^{2-}$, $[\text{trans-PtCl}_4(\text{OH})_2]^{2-}$, and $[\text{mer-PtCl}_3(\text{OH})_3]^{2-}$ species showed relatively higher absolute percentage deviations of 15.0, 10.6, 16.2, and 10.4%, respectively, while in the remaining $[\text{PtCl}_n(\text{OH})_{6-n}]^{2-}$ ($n = 0-6$) complexes the mean absolute percentage deviations are lower than 4.3%. For $[\text{PtCl}_5(\text{OH})]^{2-}$, $[\text{cis-PtCl}_4(\text{OH})_2]^{2-}$, $[\text{trans-PtCl}_4(\text{OH})_2]^{2-}$, and $[\text{mer-PtCl}_3(\text{OH})_3]^{2-}$, the error bars of the calculated from the experimental values observed are found to be 100, 136, 205, and 191 ppm, respectively. The higher mean absolute percentage deviations and error bars observed for the $[\text{PtCl}_5(\text{OH})]^{2-}$, $[\text{cis-PtCl}_4(\text{OH})_2]^{2-}$, $[\text{trans-PtCl}_4(\text{OH})_2]^{2-}$, and $[\text{mer-PtCl}_3(\text{OH})_3]^{2-}$ complexes could be attributed to the fact that $\delta_{\text{exptl}}^{195\text{Pt}}$ chemical shifts result from structures of the complexes existing in the aqueous solutions differing from the optimized structures calculated by the PBE0/SARC-ZORA(Pt) U 6-31 + G(d)(E)/SMD computational protocol. One could expect that concentration, counter-ions, pH, ionic strength, and solvent affect the structures of $[\text{PtCl}_5(\text{OH})]^{2-}$, $[\text{cis-PtCl}_4(\text{OH})_2]^{2-}$, $[\text{trans-PtCl}_4(\text{OH})_2]^{2-}$, and $[\text{mer-PtCl}_3(\text{OH})_3]^{2-}$, but all these factors could not be taken into account in the calculations. The better performance of the SMD compared to the PCM solvation model in calculation of the $\delta^{195\text{Pt}}$ chemical shifts of the $[\text{PtCl}_n(\text{OH})_{6-n}]^{2-}$ ($n = 0-6$) complexes could be attributed to the fact that SMD does not rely on a specifically developed charge model; the descriptors

required by the SMD solvation model are the dielectric constant, refractive index, and bulk surface tension, Abraham's hydrogen bond acidity and basicity, aromaticity, and *electronegative halogenicity*, while the PCM solvation model is based upon the idea of generating multiple overlapping spheres for each of the atoms within the molecule inside of a dielectric continuum and thereby does not account for the cavitation or dispersion–repulsion energies [30, 31].

The excellent performance of the PBE0/SARC-ZORA(Pt) U 6-31 + G(d)(E)/SMD computational protocol in the calculation of the $\delta^{195}\text{Pt}$ chemical shifts of the $[\text{PtCl}_n(\text{OH})_{6-n}]^{2-}$ ($n = 0-6$) complexes is further corroborated from the plots of $\delta_{\text{calcd}}(^{195}\text{Pt})$ versus $\delta_{\text{exptl}}(^{195}\text{Pt})$ chemical shifts shown in figure 2. Figure 2 shows that the best linear relationship between the experimental and calculated $\delta^{195}\text{Pt}$ chemical shifts is that obtained by the PBE0/SARC-ZORA(Pt) U 6-31 + G(d)(E)/SMD computational protocol ($\delta_{\text{exptl}} = 1.008 \delta_{\text{calcd}} - 102$ with $R^2 = 0.99$). The calculated δ_{calcd} values are typically 103% of the experimental ones (the linear relationship is $\delta_{\text{calcd}}(^{195}\text{Pt}) = 1.03 \delta_{\text{exptl}}(^{195}\text{Pt})$ with $R^2 = 0.99$). Noteworthy is also the good linear relationship between $\delta_{\text{calcd}}^{195}\text{Pt}$ and Q_{Pt} ($R^2 = 0.903$) for the complete set of the $[\text{PtCl}_n(\text{OH})_{6-n}]^{2-}$ ($n = 0-6$) complexes (figure 3) when calculations were performed employing the PBE0/SARC-ZORA(Pt) U 6-31 + G(d)(E)/SMD computational protocol ($\delta_{\text{calcd}} = 4619.1 Q_{\text{Pt}} - 456.03$ with $R^2 = 0.966$).

Taking into account that the electron density on Pt is primarily determined by the coordination environment (coordination sphere) of the octahedral $[\text{PtCl}_n(\text{OH})_{6-n}]^{2-}$ ($n = 0-6$) complexes, the excellent correlation of $\delta_{\text{calcd}}^{195}\text{Pt}$ with the natural atomic charge Q_{Pt} reveals that the PBE0/SARC-ZORA(Pt) U 6-31 + G(d)(E)/SMD computational protocol

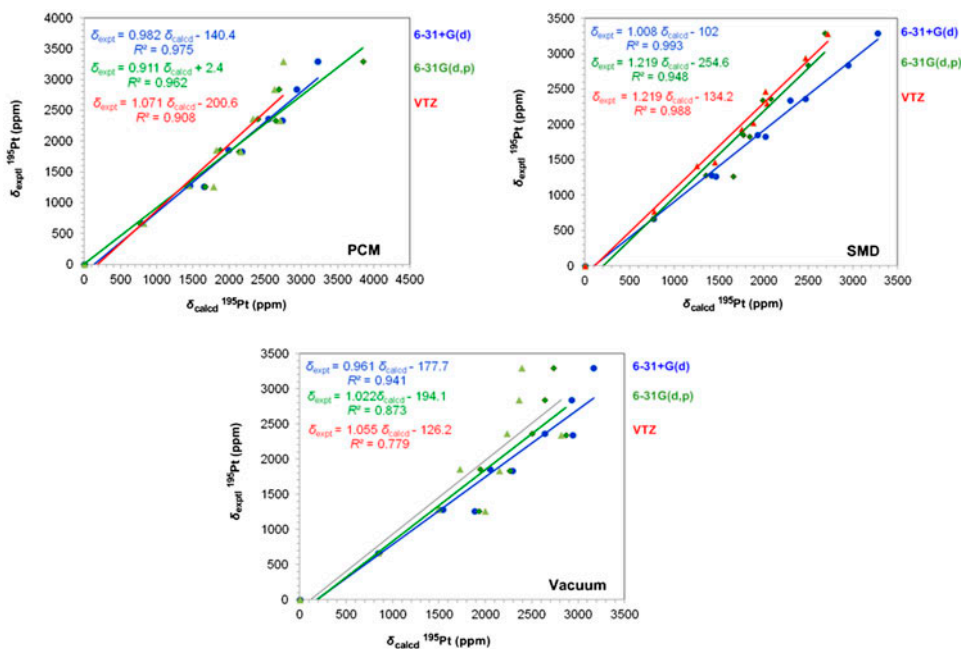


Figure 2. Linear plots of the calculated $\delta_{\text{calcd}}(^{195}\text{Pt})$ vs. experimental $\delta_{\text{exptl}}(^{195}\text{Pt})$ chemical shifts for the $[\text{PtCl}_n(\text{OH})_{6-n}]^{2-}$ ($n = 0-6$) complexes. $\delta_{\text{calcd}}(^{195}\text{Pt})$ chemical shifts were computed at all computational protocols tested.

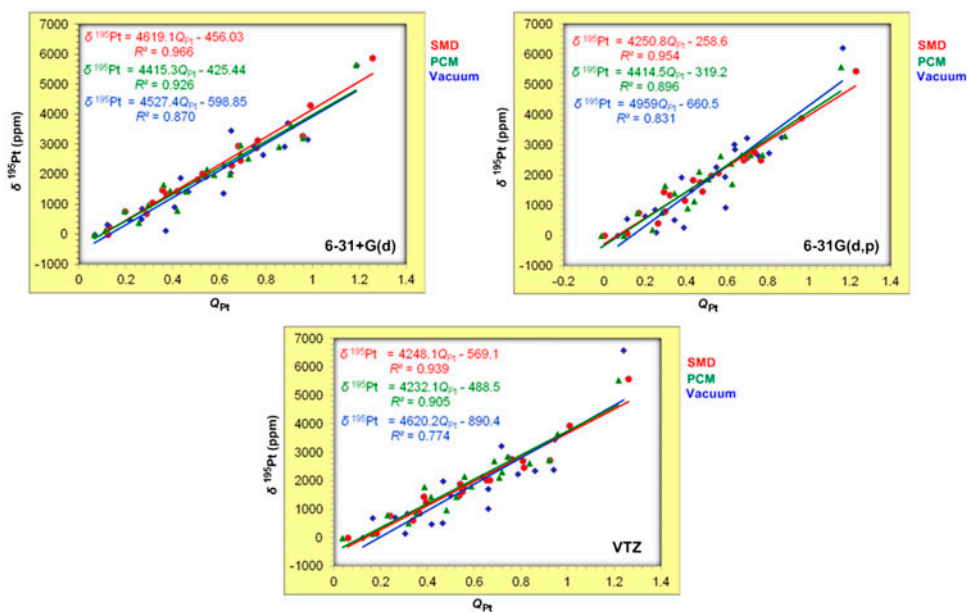


Figure 3. Linear plots of $\delta_{\text{calcd}}(^{195}\text{Pt})$ vs. Q_{Pt} for the $[\text{PtCl}_n(\text{OH})_{6-n}]^{2-}$ ($n = 0-6$) complexes calculated by the computational protocols tested.

affords structures for the $[\text{PtCl}_n(\text{OH})_{6-n}]^{2-}$ ($n = 0-6$) complexes close to the structures existing in the aqueous alkaline solutions of $[\text{PtCl}_6]^{2-}$.

The optimized geometries of the $[\text{PtCl}_n(\text{OH})_{6-n}]^{2-}$ ($n = 0-6$) complexes calculated by the above computational protocol are given in figure S3. The estimated Pt–O bond distances for OH^- *trans* to Cl^- are 2.032–2.047 Å, while for OH^- *trans* to OH^- are 2.053–2.064 Å, illustrating the higher *trans* effect of OH^- than Cl^- ligands. The higher *trans* effect of OH^- than Cl^- ligands is also reflected on the Pt–Cl bond distances, which are 2.410–2.420 Å for the Pt–Cl bond *trans* to OH^- ligand and 2.385–2.394 Å for the Pt–Cl bond in *trans* position to Cl^- ligand.

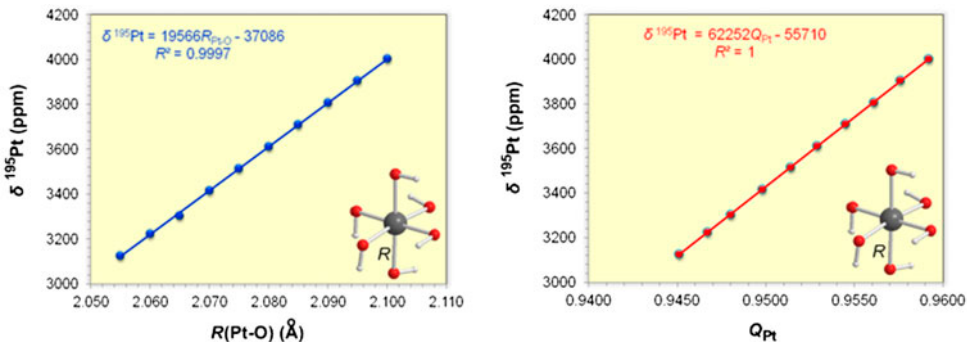


Figure 4. $\delta^{195}\text{Pt}$ vs. $R(\text{Pt}-\text{O})$ and δ^{195} vs. Q linear relationships for the $[\text{Pt}(\text{OH})_6]^{2-}$ complex calculated at the PBE0/SARC-ZORA(Pt) U 6-31 + G(d)(O)/SMD level in aqueous solutions.

Next we investigated how small changes in the $R(\text{Pt}-\text{O})$ bond distances affect the $\delta^{195}\text{Pt}$ chemical shifts and the electron density on Pt of $[\text{Pt}(\text{OH})_6]^{2-}$ employing the PBE0/SARC-ZORA(Pt) U 6-31 + G(d)(O)/SMD computational protocol. The results obtained are given in table S2, while plots of the $\delta^{195}\text{Pt}$ versus $R(\text{Pt}-\text{O})$ and $\delta^{195}\text{Pt}$ versus Q_{Pt} correlations are shown in figure 4.

Excellent linear relationships are obtained for $\delta^{195}\text{Pt}$ versus $R(\text{Pt}-\text{O})$ and $\delta^{195}\text{Pt}$ versus Q_{Pt} . An inspection of figure 4 and table S2 reveals that very small changes in the Pt–O bond distances have significant influence on the computed $\delta^{195}\text{Pt}$ chemical shifts of $[\text{Pt}(\text{OH})_6]^{2-}$. In effect, an increase of the Pt–O bond distance by 0.005 Å (5 mÅ) is accompanied by a downfield shift of 97 ppm which is translated to a downfield shift increment of 19.4 ppm mÅ⁻¹. It should be noticed that the incremental increase of the Pt–O bond distance causes a decrease (increase of Q_{Pt}) of the electron density on the central Pt and consequently the downfield shift of $\delta^{195}\text{Pt}$ chemical shifts.

A plot of the calculated $\delta^{195}\text{Pt}$ chemical shifts of the $[\text{PtCl}_n(\text{OH})_{6-n}]^{2-}$ ($n = 0-6$) complexes as a function of the number of the hydroxide ligands (figure 5) gives an excellent second-order polynomial relationship $\delta^{195}\text{Pt} = -34.9n^2 + 745.5n + 42.3$ ($R^2 = 0.995$), which slightly deviates from the linear relationship $\delta^{195}\text{Pt} = 535.9n + 251.9$ ($R^2 = 0.980$).

According to the second-order polynomial relationship, the sequential substitution of a chloride by hydroxide causes an incremental downfield shift of 70 ppm per each step of substitution with the first substitution introducing a downfield shift of 711 ppm. The lowering of the incremental downfield shift as the number of substitution step increases might be due to different coordination environment of the Pt(IV) complexes involving an increased number of OH⁻ ligands. From the linear relationship, an average incremental downfield shift of 536 ppm is observed for each individual substitution.

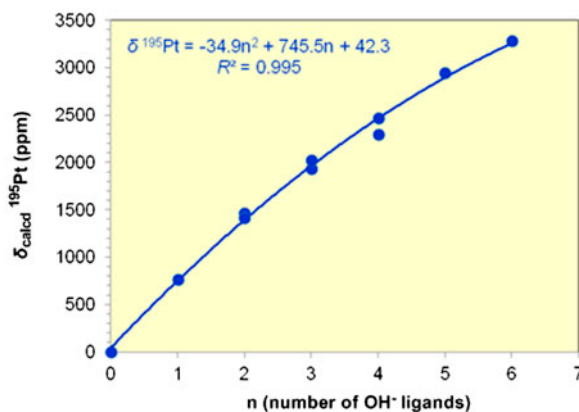


Figure 5. Plot of $\delta_{\text{calcd}}^{195}\text{Pt}$ chemical shifts of the $[\text{PtCl}_n(\text{OH})_{6-n}]^{2-}$ ($n = 0-6$) complexes as a function of the number of the hydroxide ligands calculated at the PBE0/SARC-ZORA(Pt) U 6-31 + G(d)(O) level in aqueous solutions combined with the SMD solvation model.

Table 3. ^{195}Pt -NMR chemical shifts (in ppm) for the $[\text{PtCl}_n(\text{H}_2\text{O})_{6-n}]^{4-n}$ ($n = 1-6$) complexes obtained upon stepwise substitution of Cl^- by H_2O ligands, percent deviation, Dev (%), and error bars (in ppm) calculated at the GIAO-PBE0/SARC-ZORA(Pt) U 6-31 + G(d)(Cl) and GIAO-PBE0/SARC-ZORA(Pt)U 6-31G(d,p)(Cl) (figures in parentheses) levels in aqueous solution employing the PCM and SMD solvation models.

Compound	$\delta_{\text{calcd}}^{195}\text{Pt}$		$\delta_{\text{exptl}}^{195}\text{Pt}^a$	Dev (%)		Error bars	
	PCM	SMD		PCM	SMD	PCM	SMD
$[\text{PtCl}_5(\text{OH}_2)]^-^b$	468 (468)	532 (546)	504	-7.1 (-7.1)	5.6 (8.3)	36 (36)	28 (42)
$[\text{cis-PtCl}_4(\text{OH}_2)_2]^c$	672 (684)	995 (944)	1005	-33.1 (-31.9)	-1.0 (-6.1)	333 (321)	10 (61)
$[\text{trans-PtCl}_4(\text{OH}_2)_2]$	983 (772)	1051 (818)	1126	-12.7 (-31.4)	-6.7 (-27.4)	143 (354)	75 (308)
$[\text{fac-PtCl}_3(\text{OH}_2)_3]^+$	794 (913)	1454 (1168)	1500	-47.1 (-39.1)	-3.1 (-22.1)	706 (587)	46 (332)
$[\text{mer-PtCl}_3(\text{OH}_2)_3]^+$	1439 (1145)	1817 (1471)	1603	-10.2 (-28.6)	13.3 (-8.2)	164 (458)	214 (132)
$[\text{cis-PtCl}_2(\text{OH}_2)_4]^{2+}$	2007 (1727)	2887 (2587)	2125	-5.6 (-18.7)	35.9 (21.7)	118 (396)	762 (462)
$[\text{trans-PtCl}_2(\text{OH}_2)_4]^{2+}$	2982 (2675)	3130 (2753)	2208	35.1 (21.2)	41.8 (24.7)	774 (467)	922 (545)
$[\text{PtCl}(\text{OH}_2)_5]^{3+}$	3630 (3311)	4300 (3900)	2640	37.5 (25.4)	62.9 (47.7)	990 (671)	1660 (1260)
$[\text{Pt}(\text{OH}_2)_6]^{4+}$	5658 (5584)	5882 (5437)	3329	70.0 (67.7)	76.7 (63.3)	2329 (2255)	2553 (2108)

^aFrom Ref. [3].

^bReferenced to $[\text{HPtCl}_6]^-$.

^cReferenced to $\text{cis-H}_2\text{PtCl}_6$.

3.3. ^{195}Pt -NMR chemical shifts of the $[\text{PtCl}_n(\text{OH}_2)_{6-n}]^{4-n}$ ($n = 1-6$) complexes in aqueous solutions

^{195}Pt -NMR chemical shifts for all possible $[\text{PtCl}_n(\text{OH}_2)_{6-n}]^{4-n}$ ($n = 1-6$) complexes, referenced to $[\text{PtCl}_6]^{2-}$, calculated at the GIAO-PBE0/SARC-ZORA(Pt) U BS(E) level in aqueous solutions employing the PCM and SMD solvation models are compiled in table 3.

An inspection of the calculated $\delta_{\text{calcd}}^{195}\text{Pt}$ and experimental $\delta_{\text{exptl}}^{195}\text{Pt}$ chemical shifts (table 3) reveals the excellent performance of the PBE0/SARC-ZORA(Pt) U 6-31 + G(d)(E)/SMD computational protocol for the evaluation of the $\delta^{195}\text{Pt}$ chemical shifts of $[\text{PtCl}_n(\text{OH}_2)_{6-n}]^{4-n}$ ($n = 3-5$) complexes giving the lower mean absolute percentage deviation of the calculated from the experimental values (4.1%) and the lower mean error bar of 40 ppm. However, for $[\text{mer-PtCl}_3(\text{OH}_2)_3]^+$, the percentage deviation was 13.3% and the error bar 214 ppm. For $[\text{PtCl}_n(\text{OH}_2)_{6-n}]^{4-n}$ ($n = 0-2$), all computational protocols assessed failed to predict $\delta^{195}\text{Pt}$ chemical shifts comparable to experimental values. The mean absolute percentage deviations of the calculated from the experimental values are found in the range of 29.6–60.4% and the error bars range from 762 to 2553 ppm. The high mean absolute percentage deviations observed for the $[\text{PtCl}_n(\text{OH}_2)_{6-n}]^{4-n}$ ($n = 0-2$) complexes indicate that the experimentally determined $\delta^{195}\text{Pt}$ chemical shifts result from different structures of the complexes existing in the aqueous hydrochloric acid solutions, where counter-anions surround the positively charged complexes from the optimized structures of the authentic “free” cationic complexes.

To probe if counter-anion effects on the ^{195}Pt -NMR chemical shifts of the highly positive charged complexes could improve the results, reducing the mean absolute percentage deviation of the calculated from the experimental values, we calculated the ^{195}Pt -NMR chemical shifts of the $[\text{PtCl}_n(\text{H}_2\text{O})_{6-n}]\text{Cl}_{4-n}$ ($n = 0-2$) complexes in aqueous solutions at

Table 4. ¹⁹⁵Pt-NMR chemical shifts (in ppm) of octahedral [PtCl_n(H₂O)_{6-n}]Cl_{4-n} (*n* = 0–2) complexes referenced to K₂[PtCl₆], Dev (%), and error bars (in ppm) calculated at the GIAO-PBE0/SARC-ZORA (Pt) U 6-31G(d,p)(E) and GIAO-PBE0/SARC-ZORA(Pt)U 6-31 + G(d)(E) (figures in parentheses) levels in aqueous solution augmented with the PCM solvation model.

Compound	$\delta^{195}\text{Pt}$		Dev (%)	Error bars
	Calcd	Exptl		
K ₂ [PtCl ₆]	-1224 (-1127) ^a	0		
<i>cis</i> -[PtCl ₂ (OH ₂) ₄]Cl ₂	2032 (2026)	2125	-4.4 (-4.7)	93 (99)
<i>trans</i> -[PtCl ₂ (OH ₂) ₄]Cl ₂	2354 (2423)	2208	6.6 (9.7)	146 (215)
[PtCl(OH ₂) ₅]Cl ₃	2845 (2907)	2640	7.8 (10.1)	205 (267)
		2795 ^b	1.8 (4.0)	50 (112)
[Pt(OH ₂) ₆]Cl ₄	3743 (3849)	3329	12.4 (15.6)	414 (520)

^a σ^{iso} ¹⁹⁵Pt magnetic shieldings are given for the K₂[PtCl₆] reference compound.

^bExperimental value taken from Ref. [47].

the GIAO-PBE0/SARC-ZORA(Pt) U BS(E) (BS = 6-31G(d,p) or 6-31 + G(d)) level in aqueous solutions employing the PCM solvation model (table 4). The GIAO-PBE0/SARC-ZORA(Pt) U BS(E) (BS = 6-31 + G(d) or 6-31G(d,p)) computational protocol augmented with the SMD solvation model performed worst and, therefore, the results obtained have not been included in table 4, but are given in table S3. Table 4 shows that counter-anion effects strongly contribute to the ¹⁹⁵Pt-NMR chemical shifts of the highly positively charged complexes with a spectacular improvement of the calculated ¹⁹⁵Pt-NMR chemical shifts, reducing drastically the mean absolute percentage deviation of the calculated from the experimental values. For example counter-anion effect on the ¹⁹⁵Pt-NMR chemical shifts of the [Pt(H₂O)₆]⁴⁺ species improves drastically the calculated ¹⁹⁵Pt-NMR chemical shifts, reducing the mean absolute percentage deviation of the calculated from the experimental values from 67.7% to 12.4% and the error bar from 2255 to 414 ppm. Analogous improvements of the calculated ¹⁹⁵Pt-NMR chemical shifts are observed for the rest of the highly positively charged complexes given in table 4.

The optimized geometries of [PtCl_n(H₂O)_{6-n}]Cl_{4-n} (*n* = 0–2) complexes calculated by the PBE0/SARC-ZORA(Pt) U 6-31G(d,p)(N,O,H)/PCM computational protocol are given in figure S4. Notice that the counter-anions affect the coordination sphere of the highly

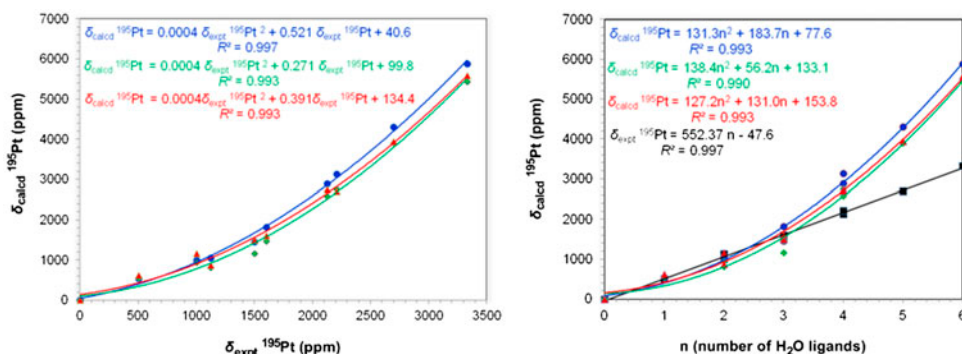


Figure 6. Second-order polynomial plots of $\delta_{\text{calcd}}^{195}\text{Pt}$ vs. $\delta_{\text{exptl}}^{195}\text{Pt}$ chemical shifts and $\delta_{\text{calcd}}^{195}\text{Pt}$ chemical shifts vs. number of coordinated H₂O ligands for the [PtCl_n(OH₂)_{6-n}]⁴⁻ⁿ (*n* = 1–6) complexes. $\delta_{\text{calcd}}^{195}\text{Pt}$ chemical shifts were computed at all assessed computational protocols.

positively charged complexes forming a second coordination shell through hydrogen bond formation with the coordinated H₂O ligands. The second coordination shell influences the electron density distribution on the Pt and consequently the ¹⁹⁵Pt-NMR chemical shifts.

A clear picture for the performance of the computational protocols assessed is also provided by plots of $\delta_{\text{calcd}}^{195\text{Pt}}$ versus $\delta_{\text{exptl}}^{195\text{Pt}}$ chemical shifts and $\delta_{\text{calcd}}^{195\text{Pt}}$ versus n (number of coordinated H₂O ligands) shown in figure 6. Figure 6 shows that the best second-order polynomial relationship between the experimental and calculated $\delta^{195\text{Pt}}$ chemical shifts is that obtained by the PBE0/SARC-ZORA(Pt) U 6-31 + G(d)(E)/SMD computational protocol ($\delta_{\text{calcd}} = 0.0004 \delta_{\text{exptl}}^2 + 0.521 \delta_{\text{exptl}} - 40.6$ with $R^2 = 0.997$). Noteworthy are the large deviations of $\delta_{\text{calcd}}^{195\text{Pt}}$ from $\delta_{\text{exptl}}^{195\text{Pt}}$ observed for the positively charged $[\text{PtCl}_n(\text{OH}_2)_{6-n}]^{4-n}$ ($n = 0-2$) complexes shown in the plot of $\delta_{\text{calcd}}^{195\text{Pt}}$ chemical shifts as a function of the number of coordinated H₂O ligands (figure 6).

For the first four members of the $[\text{PtCl}_n(\text{OH}_2)_{6-n}]^{4-n}$ ($n = 0-3$) complexes, an excellent linear relationship of $\delta_{\text{calcd}}^{195\text{Pt}}$ versus n is obtained ($\delta_{\text{calcd}}^{195\text{Pt}} = 520.3n + 2.46$; $R^2 = 0.992$). According to this relationship, the sequential substitution of a chloride by the H₂O ligand causes an average incremental downfield shift of 521 ppm ($\delta_{\text{calcd}}^{195\text{Pt}} = 521.3n$; $R^2 = 0.992$) per each step of substitution (compare with the average incremental downfield shift of 536 ppm for substitution of a chloride by the OH⁻ ligand). According to the aforementioned linear relationship, one could predict $\delta_{\text{calcd}}^{195\text{Pt}}$ chemical shifts for the positively charged $[\text{PtCl}_2(\text{OH}_2)_4]^{2+}$ (*cis*- and *trans*-isomers), $[\text{PtCl}(\text{OH}_2)_5]^{3+}$, and $[\text{Pt}(\text{OH}_2)_6]^{4+}$ complexes of 2085, 2607, and 3124 ppm, respectively. Noteworthy, these values are very close to the experimental ones (mean absolute percentage deviations of 1.9–5.6, 1.3, and 6.2% for the $[\text{PtCl}_2(\text{OH}_2)_4]^{2+}$ (*cis*- and *trans*-isomers), $[\text{PtCl}(\text{OH}_2)_5]^{3+}$, and $[\text{Pt}(\text{OH}_2)_6]^{4+}$ complexes, respectively).

The $[\text{PtCl}_n(\text{OH}_2)_{6-n}]^{4-n}$ ($n = 1-6$) complexes are more shielded compared to $[\text{PtCl}_n(\text{OH})_{6-n}]^{2-n}$ ($n = 1-6$) complexes, since the H₂O ligands are weaker donors than the OH⁻ ligands. Accordingly, the Pt–OH₂ bond distances are longer than the Pt–OH ones and Pt acquires higher natural atomic charge Q_{Pt} in $[\text{PtCl}_n(\text{OH}_2)_{6-n}]^{4-n}$ ($n = 1-6$) than $[\text{PtCl}_n(\text{OH})_{6-n}]^{2-n}$ ($n = 1-6$) complexes. Thus, for example, the Pt–OH₂ bond distance in $[\text{PtCl}_5(\text{OH}_2)]^+$ is 2.171 Å, while the Pt–OH bond distance in $[\text{PtCl}_5(\text{OH})]^{2-}$ is 2.047 Å. Moreover, the stronger *trans*-effect of the OH⁻ than the H₂O ligands results in longer

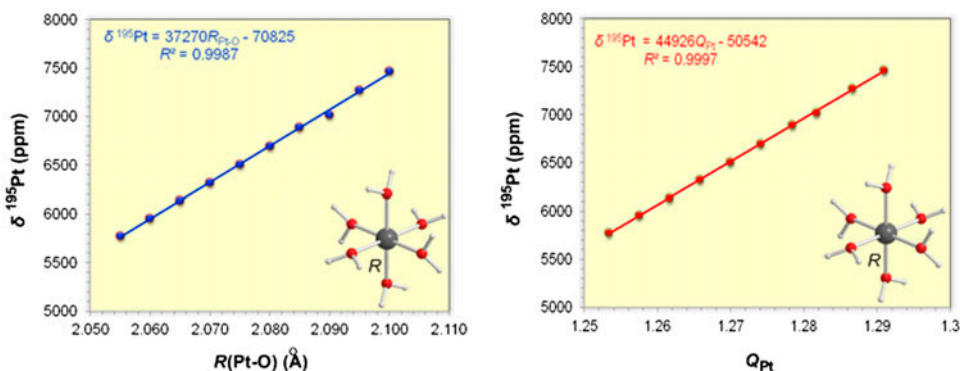


Figure 7. $\delta^{195\text{Pt}}$ vs. $R(\text{Pt}-\text{O})$ and $\delta^{195\text{Pt}}$ vs. Q_{Pt} linear relationships for $[\text{Pt}(\text{OH}_2)_6]^{4+}$ calculated with the PBE0/SARC-ZORA(Pt) U 6-31 + G(d)(O)/SMD computational protocol.

trans-Pt–Cl bonds in $[\text{PtCl}_n(\text{OH})_{6-n}]^{2-}$ ($n = 1-6$) than the $[\text{PtCl}_n(\text{OH}_2)_{6-n}]^{4-n}$ ($n = 1-6$) complexes. For example, the Pt–Cl bond distance *trans* to H_2O ligand in $[\text{PtCl}_5(\text{OH}_2)]^-$ is 2.319 Å, while the Pt–Cl bond distance *trans* to OH^- in $[\text{PtCl}_5(\text{OH})]^{2-}$ is 2.412 Å. Details on the structural parameters of the optimized geometries of the $[\text{PtCl}_n(\text{OH}_2)_{6-n}]^{4-n}$ ($n = 1-6$) complexes along with the estimated natural atomic charge, Q_{Pt} calculated at the PBE0/SARC-ZORA(Pt) U 6-31 + G(d) (Cl,O,H) level combined with the SMD solvation model are given in figure S5.

We further investigated the effect of small variations of the $R(\text{Pt}-\text{O})$ bond distances on the $\delta^{195}\text{Pt}$ chemical shifts and the natural atomic charge on Pt Q_{Pt} of $[\text{Pt}(\text{OH}_2)_6]^{4+}$ employing the PBE0/SARC-ZORA(Pt) U 6-31 + G(d)(O)/SMD computational protocol. The results are given in table S4, while plots of the $\delta^{195}\text{Pt}$ versus $R(\text{Pt}-\text{O})$ and $\delta^{195}\text{Pt}$ versus Q_{Pt} correlations are shown in figure 7.

Excellent linear relationships are obtained for $\delta^{195}\text{Pt}$ versus $R(\text{Pt}-\text{O})$, $\delta^{195}\text{Pt}$ versus Q_{Pt} , and Q_{Pt} versus $R(\text{Pt}-\text{O})$ correlations. Perusal of table S4 and figure 7 reveals that very small changes in the $R(\text{Pt}-\text{O})$ bond distances have a significant influence on the computed $\delta^{195}\text{Pt}$ chemical shifts of the $[\text{Pt}(\text{OH}_2)_6]^{4+}$ complex. In effect, an increase of the Pt–O bond distance by 5 mÅ is accompanied by a downfield shift of 188 ppm which is translated to a downfield shift increment of 37.6 ppm mÅ $^{-1}$. Noteworthy is the higher sensitivity of the $\delta^{195}\text{Pt}$ chemical shifts to small changes in the $R(\text{Pt}-\text{O})$ bond distances of $[\text{Pt}(\text{OH}_2)_6]^{4+}$ than $[\text{Pt}(\text{OH})_6]^{2-}$ (37.6 vs. 19.4 ppm mÅ $^{-1}$). It should be noticed once more that the incremental increase of the Pt–O bond distance causes a decrease (increase of Q_{Pt}) of the electron density on the Pt and consequently the downfield shift of $\delta^{195}\text{Pt}$ chemical shifts (figure 7).

4. Conclusion

The successful computation of accurate ^{195}Pt chemical shifts for the series of all possible hydrolysis products of $[\text{PtCl}_6]^{2-}$ in acidic and alkaline aqueous solutions was achieved employing the GIAO-PBE0/SARC-ZORA(Pt) U BS(E) (BS = 6-31 + G(d) or 6-31G(d,p) basis set for *E*) computational protocols augmented either with the SMD or the PCM solvation models. Important results are summarized as follows:

- (1) The GIAO-PBE0/SARC-ZORA(Pt) U 6-31 + G(d)(E)/SMD (*E* = main group element) computational protocol performs the best for calculation of the ^{195}Pt -NMR chemical shifts of octahedral $[\text{PtCl}_n(\text{OH})_{6-n}]^{2-}$ and $[\text{PtCl}_n(\text{OH}_2)_{6-n}]^{4-n}$ ($n = 1-6$) complexes existing in alkaline and acidic solutions of $[\text{PtCl}_6]^{2-}$. The mean absolute percentage deviation of the calculated from the experimental values are 7.4 and 5.9% for the $[\text{PtCl}_n(\text{OH})_{6-n}]^{2-}$ and $[\text{PtCl}_n(\text{OH}_2)_{6-n}]^{4-n}$ ($n = 1-6$) complexes, respectively.
- (2) The excellent linear plots of $\delta_{\text{calcd}}(^{195}\text{Pt})$ chemical shifts versus $\delta_{\text{exptl}}(^{195}\text{Pt})$ chemical shifts and $\delta_{\text{calcd}}(^{195}\text{Pt})$ versus the natural atomic charge Q_{Pt} for the octahedral $[\text{PtCl}_n(\text{OH})_{6-n}]^{2-}$ and $[\text{PtCl}_n(\text{OH}_2)_{6-n}]^{4-n}$ ($n = 1-6$) complexes illustrate the good performance of the proposed computational protocols.
- (3) The good performance of the PBE0/SARC-ZORA(Pt) U 6-31G(d,p)(N,O,H)/PCM computational protocol is also imprinted on the plots of $\delta_{\text{calcd}}^{195}\text{Pt}$ versus $\delta_{\text{exptl}}^{195}\text{Pt}$ chemical shifts and $\delta_{\text{calcd}}^{195}\text{Pt}$ versus n (number of coordinated H_2O ligands) giving the best second-order polynomial relationship between the experimental and calculated $\delta^{195}\text{Pt}$ chemical shifts.

- (4) Counter-anion effects strongly contribute to the ^{195}Pt -NMR chemical shifts of the highly positive charged complexes improving drastically the accuracy of the calculated ^{195}Pt -NMR chemical shifts.
- (5) The crucial role of the coordination environment (coordination sphere) on the electron density of the Pt of the octahedral $[\text{PtL}_n(\text{OH})_{6-n}]^{2-}$ and $[\text{PtL}_n(\text{OH}_2)_{6-n}]^{4-n}$ ($L = \text{Cl}^-$ or NO_3^- ; $n = 1-6$) complexes and consequently on the calculated δ ^{195}Pt chemical shifts is mirrored in the excellent linear plots of δ_{calcd} ^{195}Pt chemical shifts versus Pt–Cl bond distance and δ_{calcd} ^{195}Pt chemical shifts versus Pt–O bond distance obtained for $[\text{PtCl}_6]^{2-}$, $[\text{Pt}(\text{OH})_6]^{2-}$, and $[\text{Pt}(\text{OH}_2)_6]^{4+}$. An increase of the Pt–Cl and Pt–O bond distances by 0.001 Å (1 mÅ) is accompanied by a downfield shift increment of 17.0, 19.4, and 37.6 ppm mÅ $^{-1}$ for $[\text{PtCl}_6]^{2-}$, $[\text{Pt}(\text{OH})_6]^{2-}$, and $[\text{Pt}(\text{OH}_2)_6]^{4+}$, respectively.
- (6) Due to the high sensitivity of the computed σ^{iso} ^{195}Pt magnetic shielding tensor elements for the reference standards, accurate δ ^{195}Pt chemical shifts could be predicted if the calculations of the σ^{iso} ^{195}Pt magnetic shielding for the appropriate reference standard are performed strictly under the same conditions.

Supplementary material

Structural and ^{195}Pt -NMR parameters of the anionic $[\text{PtCl}_6]^{2-}$, $[\text{HPtCl}_6]^-$, and neutral $\text{H}_2[\text{PtCl}_6]$ reference standards and the octahedral $[\text{PtCl}_n(\text{OH})_{6-n}]^{2-}$, $[\text{PtL}_n(\text{OH}_2)_{6-n}]^{4-n}$ ($n = 1-6$), and $[\text{PtCl}_n(\text{H}_2\text{O})_{6-n}]\text{Cl}_{4-n}$ ($n = 0-2$) complexes (figures S1–S5); variation of σ^{iso} ^{195}Pt (in ppm), and natural atomic charge Q_{Pt} , with respect to the variation of the $R(\text{Pt}–\text{Cl})$ bond distances (in Å) in the anionic $[\text{PtCl}_6]^{2-}$ reference compound (table S1); variation of δ ^{195}Pt (in ppm) referenced to $[\text{PtCl}_6]^{2-}$ complex and natural atomic charge Q_{Pt} , as a function of the $R(\text{Pt}–\text{O})$ bond distances (in Å) in $[\text{Pt}(\text{OH})_6]^{2-}$ (table S2), the ^{195}Pt -NMR chemical shifts of $[\text{PtCl}_n(\text{H}_2\text{O})_{6-n}]\text{Cl}_{4-n}$ ($n = 0-2$) complexes (table S3); variation of δ ^{195}Pt (in ppm) referenced to $[\text{PtCl}_6]^{2-}$ complex and natural atomic charge Q_{Pt} , as a function of the $R(\text{Pt}–\text{O})$ bond distances (in Å) in $[\text{Pt}(\text{OH}_2)_6]^{4+}$ complex (table S4); Cartesian Coordinates and energies (in Hartrees) of the anionic $[\text{PtCl}_6]^{2-}$, $[\text{HPtCl}_6]^-$, and neutral $\text{H}_2[\text{PtCl}_6]$ reference standards and the octahedral $[\text{PtCl}_n(\text{OH})_{6-n}]^{2-}$, $[\text{PtCl}_n(\text{OH}_2)_{6-n}]^{4-n}$ ($n = 1-6$), and $[\text{PtCl}_n(\text{H}_2\text{O})_{6-n}]\text{Cl}_{4-n}$ ($n = 0-2$) complexes (table S5).

Acknowledgement

The authors are very grateful to Dr. Dimitrios A. Pantazis at Max Planck Institute for Chemical Energy Conversion for fruitful discussions.

Disclosure statement

No potential conflict of interest was reported by the authors.

Supplementary data

The supplementary data for this article is available online at <http://dx.doi.org/10.1080/00958972.2015.1083095>

References

- [1] J. Kramer, K.R. Koch. *Inorg. Chem.*, **45**, 7843 (2006).
- [2] T.M. Buslaeva, S.A. Simanova. *Russ. J. Coord. Chem.*, **25**, 151 (1999).
- [3] C. Carr, P.L. Goggin, R.J. Goodfellow. *Inorg. Chim. Acta*, **81**, L25 (1984).
- [4] L.E. Cox, D.G. Peters. *Inorg. Chem.*, **9**, 1927 (1970).
- [5] G. Bandel, M. Müllner, M. Trömel. *Z. Anorg. Allg. Chem.*, **453**, 5 (1979).
- [6] L.E. Cox, D.G. Peters, E.L. Wehry. *J. Inorg. Nucl. Chem.*, **34**, 297 (1972).
- [7] J. Kramer, K.R. Koch. *Inorg. Chem.*, **46**, 7466 (2007).
- [8] W.J. Gerber, P. Murray, K.R. Koch. *Dalton Trans.*, 4113 (2008).
- [9] P. Murray, W.J. Gerber, K.R. Koch. *Dalton Trans.*, **41**, 10533 (2012).
- [10] K.R. Koch, M.R. Burger, J. Kramer, A.N. Westra. *Dalton Trans.*, 3277 (2006).
- [11] J.C. Davis, M. Bühl, K.R. Koch. *J. Chem. Theory Comput.*, **8**, 1344 (2012).
- [12] J.C. Davis, M. Bühl, K.R. Koch. *J. Phys. Chem. A*, **117**, 8054 (2013).
- [13] I.M. Ismail, S.J.S. Kerrison, P.J. Sadler. *Chem. Commun.*, 1175 (1980).
- [14] P. Murray. A speciation study of various Pt(II) and Pt(IV) complexes including hexaaquaplatinum(IV) by means of ¹⁹⁵Pt NMR spectroscopy, in support of a preliminary study of the oxidation mechanism of various Pt(II) complexes. PhD thesis, Stellenbosch University (2012). <http://scholar.sun.ac.za>
- [15] A.C. Tsipis, I.N. Karapetsas. *Dalton Trans.*, **43**, 5409 (2014).
- [16] M.J. Frisch, G.W. Trucks, H.B. Schlegel, G.E. Scuseria, M.A. Robb, J.R. Cheeseman, G. Scalmani, V. Barone, B. Mennucci, G.A. Petersson, H. Nakatsuji, M. Caricato, X. Li, H.P. Hratchian, A.F. Izmaylov, J. Bloino, G. Zheng, J.L. Sonnenberg, M. Hada, M. Ehara, K. Toyota, R. Fukuda, J. Hasegawa, M. Ishida, T. Nakajima, Y. Honda, O. Kitao, H. Nakai, T. Vreven, J.A. Montgomery, Jr., J.E. Peralta, F. Ogliaro, M. Bearpark, J.J. Heyd, E. Brothers, K.N. Kudin, V.N. Staroverov, R. Kobayashi, J. Normand, K. Raghavachari, A. Rendell, J.C. Burant, S.S. Iyengar, J. Tomasi, M. Cossi, N. Rega, J.M. Millam, M. Klene, J.E. Knox, J.B. Cross, V. Bakken, C. Adamo, J. Jaramillo, R. Gomperts, R.E. Stratmann, O. Yazyev, A.J. Austin, R. Cammi, C. Pomelli, J.W. Ochterski, R.L. Martin, K. Morokuma, V.G. Zakrzewski, G.A. Voth, P. Salvador, J.J. Dannenberg, S. Dapprich, A.D. Daniels, O. Farkas, J.B. Foresman, J.V. Ortiz, J. Cioslowski, D.J. Fox, *Gaussian 09, Revision B.01*, Gaussian, Inc., Wallingford, CT (2010).
- [17] M. Ernzerhof, G.E. Scuseria. *J. Chem. Phys.*, **110**, 5029 (1999).
- [18] C. Adamo, V. Barone. *Chem. Phys. Lett.*, **274**, 242 (1997).
- [19] C. Adamo, V. Barone. *J. Chem. Phys.*, **110**, 6160 (1999).
- [20] C. Adamo, G.E. Scuseria, V. Barone. *J. Chem. Phys.*, **111**, 2889 (1999).
- [21] C. Adamo, V. Barone. *Theor. Chem. Acc.*, **105**, 169 (2000).
- [22] V. Vetere, C. Adamo, P. Maldivi. *Chem. Phys. Lett.*, **325**, 99 (2000).
- [23] J.P. Perdew, K. Burke, M. Ernzerhof. *Phys. Rev. Lett.*, **77**, 3865 (1996).
- [24] D.A. Pantazis, X.-Y. Chen, C.R. Landis, F. Neese. *J. Chem. Theory Comput.*, **4**, 908 (2008).
- [25] EMSL basis set exchange. Available online at: <https://bse.pnl.gov/bse/portal> (accessed 08 January 2013).
- [26] D. Paschoal, B.L. Marcial, J.F. Lopes, W.B. De Almeida, H.F. Dos Santos. *J. Comput. Chem.*, **33**, 2292 (2012).
- [27] D.A. Pantazis. Personal communication.
- [28] O. Matsuoka, S. Huzinaga. *Chem. Phys. Lett.*, **140**, 567 (1987).
- [29] E.V.R. de Castro, F.E. Jorge. *J. Chem. Phys.*, **108**, 5225 (2009).
- [30] J. Tomasi, B. Mennucci, R. Cammi. *Chem. Rev.*, **105**, 2999 (2005).
- [31] A.V. Marenich, C.J. Cramer, D.G. Truhlar. *J. Phys. Chem. B*, **113**, 6378 (2009).
- [32] R. Ditchfield. *Mol. Phys.*, **27**, 789 (1974).
- [33] J. Gauss. *J. Chem. Phys.*, **99**, 3629 (1993).
- [34] R.K. Harris, E.D. Becker, S.M. Cabral de Menezes, R. Goodfellow, P. Granger. *Pure Appl. Chem.*, **73**, 1795 (2001).
- [35] P.S. Pregosin. *Coord. Chem. Rev.*, **44**, 247 (1982).
- [36] M. Sterzel, J. Autschbach. *Inorg. Chem.*, **45**, 3316 (2006).
- [37] L.A. Truflandier, J. Autschbach. *J. Am. Chem. Soc.*, **132**, 3472 (2010).
- [38] W.A. Spieker, J. Liu, J.T. Miller, A.J. Kropf, J.R. Regalbutto. *Appl. Catal., A*, **232**, 219 (2002).
- [39] R.W. Maatman, C.J. Addink. *J. Catal.*, **15**, 210 (1969).
- [40] X. Ribas, J.C. Dias, J. Morgado, K. Wurst, M. Almeida, T. Parella, J. Veciana, C. Rovira. *Angew. Chem. Int. Ed.*, **43**, 4049 (2004).
- [41] B. Nowak. *Solid State Nucl. Magn. Reson.*, **37**, 36 (2010).

- [42] E.P. Fowe, P. Belser, C. Daul, H. Chermette. *Phys. Chem. Chem. Phys.*, **7**, 1732 (2005).
- [43] M.R. Burger, J. Kramer, H. Chermette, K.R. Koch. *Magn. Reson. Chem.*, **48**, S38 (2010).
- [44] X. Chen, W. Chu, L. Wang, Z. Wu. *J. Mol. Struct.*, **920**, 40 (2009).
- [45] J. Schefer, D. Schwarzenbach, P. Fischer, T. Koetzle, F.K. Larsen, S. Haussühl, M. Rüdinger, G. McIntyre, H. Birkedal, H.-B. Bürgi. *Acta Crystallogr., Sect. B: Struct. Sci.*, **54**, 121 (1998).
- [46] K. Sutter, J. Autschbach. *J. Am. Chem. Soc.*, **134**, 13374 (2012).
- [47] V.P. Tarasov, V.L. Privalov, Y.A. Buslaev. *Mol. Phys.*, **35**, 1047 (1978).